

The EMC effect at low x in perturbative QCD

N.Armesto and M.A.Braun*

Departamento de Física de Partículas,
Universidade de Santiago de Compostela,
15706-Santiago de Compostela, Spain

March 1996

Abstract.

The EMC effect is studied in the perturbative QCD hard pomeron approach. In the limit $x \rightarrow 0$ and for a nucleus with a constant density the effect is found to be a function of a single variable which combines its x -, Q - and A -dependence. At large Q^2 the effect dies out as $\ln Q/Q$. At small but finite x a change in the anomalous dimension leads to a weaker Q -dependence, which almost disappears as x grows and the anomalous dimension becomes small. In this approach the nuclear structure function can be expressed directly in terms of the proton one. Calculations of the EMC effect on these lines give results which agree reasonably well to the existing experimental data for $x < 0.05$.

hep-ph/9603360
US-FT/15-96

*Visiting professor IBERDROLA; on leave of absence from the Department of High Energy Physics, University of St. Petersburg, 198904 St. Petersburg, Russia.

1 Introduction

The nature of the EMC effect at small x is well understood qualitatively. At high enough Q^2 the incoming photon splits into a $q\bar{q}$ pair which interacts with the nucleus target in the manner typical for a hadronic projectile and thus experiences absorption which makes the structure function (per nucleon) become smaller than for a free nucleon [1-5]. An alternative, though equivalent, explanation (appropriate for the reference system in which the nucleus is moving fast) is that the gluonic clouds created by different nucleons of the nucleus begin to overlap and the gluons recombine, so that their density becomes smaller [6-8]. However, as far as quantitative predictions are concerned, published results heavily depend on additional semiphenomenological assumptions and often contradict each other. In particular the Q -dependence of the effect results different in different approaches. In a serie of papers [3-5] it is argued that $q\bar{q}$ configurations of a large dimension give the dominant contribution to the absorption, which results essentially independent of Q . On the other hand in the gluon recombination approach of [6-8] the absorption is obtained as a clear higher-twist effect dying out at large Q .

In this note we calculate the nuclear structure function in perturbative QCD which seems to be applicable to the low x region. To simplify the treatment we additionally take the number of colours N_c to be very large. In this limit the low x nuclear structure function can be calculated in a closed form and results quite simple: it is given by the exchange of any number of BFKL pomerons [9] between the projectile $q\bar{q}$ pair and nucleons of the target. Corrections have the relative order of $1/N_c^2$, which may be not too bad for the physical case $N_c = 3$.

A peculiar property of the BFKL pomeron is that, due to the unperturbative rise of the anomalous dimension up to unity, the effective cross section of the coloured dipole formed by the $q\bar{q}$ pair is proportional to its transverse dimension r rather than to r^2 , as taken in [3-5]. As a result, a strong violation of scaling is predicted for the proton structure function $F_{2p}(x, Q^2)$ at low x , which should rise linearly with Q .

For the nucleus our calculations reveal that absorptive corrections due to n interactions with the target ($n \geq 2$) are indeed independent of Q , as stated in [1], and have the order m^{2-n} in the effective quark mass. However for a heavy nucleus contributions with different n obtained in this manner cancel in the sum, so that the resulting absorption results independent of the quark mass. A careful study of this result shows that contrary to the afore mentioned assertions large spatial separations of the $q\bar{q}$ pair are not singled out, its typical dimension being small and independent of Q , of the order $A^{-1/3}R_N$, where R_N is the nucleon radius. For a nucleus with a constant density inside a sphere of a radius $R_A = A^{1/3}R_0$ the

calculated EMC effect turns out to be a function of a single variable

$$z_0 = cA^{1/3} \frac{1}{Q} \left(\frac{1}{x}\right)^\Delta,$$

which combines its x -, Q - and A -dependence. The effect goes down as $\ln Q/Q$ at high Q^2 and rises with A and $1/x$ as expected, its absolute magnitude remaining relatively small up to $x \sim 10^{-6}$ and not too low Q^2 .

The asymptotic pomeron approach may only be applicable at quite small $x < 0.001$, at which the existing experimental data on $F_{2p}(x, Q^2)$ do not contradict the predicted linear rise with Q . At larger x the growth with Q is less pronounced, which indicates that the anomalous dimension of the pomeron becomes smaller and tends to zero at finite x . It turns out that the experimental data on $F_{2p}(x, Q^2)$ up to $x < 0.05$ can be well described by a subasymptotic pomeron with the effective anomalous dimension going down logarithmically in x . With this subasymptotic pomeron as an input, we have calculated the nucleon structure functions for $x < 0.05$. Comparison to the existing experimental data shows a quite reasonable agreement.

As a result of a changing anomalous dimension the Q dependence of the EMC effect results also x -dependent, becoming weaker as x grows. With the anomalous dimension close to zero, the effect becomes independent of Q , in agreement with the statements in [3-5].

2 The γ^*A scattering in the leading approximation in $1/N_c$

As is well known, in the high-colour limit all contributions to the scattering amplitude in perturbative QCD can be classified according to the topological structure of the corresponding Feynman diagrams [10,11]. The leading diagrams have the topological structure of a cylinder. For γ^* -hadron scattering they sum into a single BFKL pomeron [12]. Diagrams with more complicated topologies correspond to multipomeron exchanges with all sort of interaction between the pomerons.

For γ^* -nucleus scattering the leading diagrams in $1/N_c$ correspond to the exchange of several pomerons with their possible branchings as they propagate to the nucleus (generalized fan diagrams, Fig. 1). In the perturbative domain

$$g^2 N_c \ll 1 \tag{1}$$

only the simplest of them survive at high energies, those without branchings (Fig. 1a). Indeed the energy dependence of the two diagrams of Figs. 1a and 1b is given by $(s_1 s_2)^{2\Delta}$ and $s_1^\Delta s_2^{2\Delta}$ respectively, so that the contribution from Fig. 1a clearly dominates if s_1 is large. If, on the other hand, s_1 is finite then it continues to be dominant because in this case the contribution of Fig. 1b includes an extra factor $g^2 N_c$ not compensated by a large $\ln s$.

Thus in the dominant approximation in $1/N_c$ we have to sum only the diagrams which correspond to Fig. 1a with any number of pomerons. To do this we have to know the coupling of the projectile photon to an arbitrary (even) number of gluons, which form colourless pairs. In the high-colour limit and in the lowest order in $g^2 N_c$ this vertex has been calculated in [12]. For $2n$ gluons with momenta q_i , $i = 1, \dots, 2n$, $\sum q_i = 0$, it is given by

$$F^{(2n)}(q_{i\perp}) = ig^{2n} \left(\frac{N_c^2 - 1}{2N_c} \right)^n \int_0^1 d\alpha \int d^2r \rho(\alpha, r) \prod_{i=1}^{2n} [\exp(irq_i) - 1]. \quad (2)$$

Here $\rho(\alpha, r)$ is the (dipole) colour density created by the projectile photon as it splits into a $q\bar{q}$ pair with a part α of its longitudinal momentum carried by the quark and a transverse distance r between the quark and the antiquark. For longitudinal (L) and transverse (T) photons of virtuality Q^2 this density has been calculated in [3]:

$$\rho_L(\alpha, r) = \frac{4e^2 N_c Q^2}{(2\pi)^3} \sum_{f=1}^{N_f} Z_f^2 [\alpha(1-\alpha)]^2 K_0^2(\epsilon_f r), \quad (3)$$

$$\rho_T(\alpha, r) = \frac{e^2 N_c}{(2\pi)^3} \sum_{f=1}^{N_f} Z_f^2 \{m_f^2 K_0^2(\epsilon_f r) + [\alpha^2 + (1-\alpha)^2] \epsilon_f^2 K_1^2(\epsilon_f r)\}, \quad (4)$$

where the summation goes over flavours,

$$\epsilon_f^2 = \alpha(1-\alpha)Q^2 + m_f^2 \quad (5)$$

and m_f and Z_f are the mass and charge of the quark of flavour f .

The $2n$ gluons coupled to the vertex (2) form n pomerons as a result of their interaction. We assume that the pomerons are formed by pairs of gluons $(1, n+1)$, $(2, n+2)$ and so on. Upon reaching the nucleus each pomeron is coupled to a nucleon with a vertex analogous to (2) with $n = 1$, depending on the primed momenta q'_i and q'_{n+i} , $i = 1, \dots, n$, and involving an unknown (nonperturbative) colour density for the nucleon $\rho_N(\alpha'_i, r'_i)$. It is also clear that each pomeron has its total momentum equal to zero: $q_i + q_{n+i} = q'_i + q'_{n+i} = 0$. Then its propagator will be given by the BFKL Green function for the forward scattering [13]:

$$if(\nu, q_i, q'_i)/(N_c^2 - 1), \quad i = 1, \dots, n, \quad (6)$$

where $\nu = pq$, $q_{n+i} = -q_i$, $q'_{n+i} = -q'_i$. The factor $1/(N_c^2 - 1)$ comes from the projection onto the colourless state.

Integrations over q_i and q'_i with the exponential factors contained in the vertices transform this Green function to the coordinate space. As a function of coordinates, the BFKL Green function vanishes at the origin, so that terms with unity instead of $\exp(iq_i r)$ in (2) give no contribution. As a result each pomeron propagator turns into the coordinate Green function for the forward scattering

$$4if(\nu, r, r'_i)/(N_c^2 - 1), \quad i = 1, \dots, n, \quad (7)$$

which should be integrated over r and all r'_i with the corresponding colour densities.

One has to finally recall that each interaction with a nucleon of the target is accompanied by a nuclear profile function factor $T(b)$ giving the probability to meet a nucleon at a given impact parameter b . Also a binomial factor C_A^n should be included for n interactions.

Then in the end we arrive at the following expression for the γ^*A forward scattering amplitude with n interactions:

$$A^{(n)}(p, q) = -4i\nu C_A^n w_n \int_0^1 d\alpha \int d^2r \rho(\alpha, r) [-\sigma(r)/2]^n. \quad (8)$$

Here

$$\sigma(r) = \frac{2g^4}{(2\pi)^2} \frac{N_c^2 - 1}{N_c^2} \int_0^1 d\alpha' \int d^2r' \rho_N(\alpha', r') f(\nu, r, r') \quad (9)$$

has the meaning of the cross section for the scattering of a colour dipole formed by the $q\bar{q}$ pair of transverse dimension r off the nucleon. The factor w_n gives the total probability to find n nucleons at the same impact parameter:

$$w_n = \int d^2b T^n(b). \quad (10)$$

Evidently the amplitude (8) has an eikonal form under the sign of integration over α and r . The γ^*A total cross section is obtained as $\text{Im } A/(2\nu)$. From (8),

$$\sigma_A^{(n)} = -2C_A^n w_n \int_0^1 d\alpha \int d^2r \rho(\alpha, r) [-\sigma(r)/2]^n. \quad (11)$$

Summing over all possible numbers of interactions we find the total cross section:

$$\sigma_A = 2 \int d^2b \int_0^1 d\alpha \int d^2r \rho(\alpha, r) \left\{ 1 - [1 - (1/2)\sigma(r)T(b)]^A \right\}. \quad (12)$$

Now we turn to the cross section $\sigma(r)$ defined by (9). The explicit form of the BFKL Green function which enters (9) is [13]

$$f(\nu, r, r') = \frac{rr'}{8} \int_{-\infty}^{\infty} d\kappa \frac{\nu^{\omega(\kappa)}}{(\kappa^2 + 1/4)^2} \left(\frac{r'}{r}\right)^{2i\kappa}, \quad (13)$$

where

$$\omega(\kappa) = -(g^2 N_c / 2\pi^2) [\text{Re } \psi(1/2 + i\kappa) - \psi(1)]. \quad (14)$$

We have retained only the isotropic part, which gives the dominant contribution at high ν . At such ν small values of κ contribute in (13) for which $\omega(\kappa)$ has the form

$$\omega(\kappa) = \Delta - a\kappa^2, \quad (15)$$

where, in terms of $\alpha_s = g^2/4\pi$,

$$\Delta = (\alpha_s N_c / \pi) 4 \ln 2 \quad (16)$$

is the pomeron intercept and

$$a = (\alpha_s N_c / \pi) 14 \zeta(3). \quad (17)$$

With (15) the asymptotical expression for the Green function results

$$f(\nu, r, r')_{\nu \rightarrow \infty} \simeq 2rr' \nu^\Delta \sqrt{\frac{\pi}{a \ln \nu}} \exp\left(-\frac{\ln^2(r/r')}{a \ln \nu}\right). \quad (18)$$

As one may see from (8) and (9) characteristic values of r and r' are of the order $1/Q$ and $1/m_N$ respectively, where m_N is the nucleon mass. Then the exponential factor in (18) is close to unity, unless Q becomes so large that $\ln^2 Q \sim \ln \nu$, which we assume not to be the case. Omitting this factor we obtain

$$\sigma(r) = \mu r R_N, \quad (19)$$

where

$$R_N = \int_0^1 d\alpha' \int d^2 r' r' \rho_N(\alpha', r') \quad (20)$$

is the average transverse dimension of the nucleon and the factor μ is given by

$$\mu = \frac{16\pi\alpha_s^{3/2}}{\sqrt{14N_c\zeta(3)}} \frac{N_c^2 - 1}{N_c^2} \frac{\nu^\Delta}{\sqrt{\ln \nu}}. \quad (21)$$

It becomes large as $\nu \rightarrow \infty$.

Eqs. (12) and (19) allow in principle to calculate the $\gamma^* A$ cross section in a straightforward manner for the longitudinal and transverse photons using the densities given by (3) and (4). The nuclear structure function at low x can then be calculated as

$$F_{2A} = \frac{Q^2}{\pi e^2} [\sigma_A^{(T)} + \sigma_A^{(L)}]. \quad (22)$$

However before doing so, we have to make two important remarks.

The first one concerns the dependence of $\sigma(r)$ on r . It is proportional to r rather than to r^2 as assumed in [3-5]. This fact can be traced to the anomalous behaviour of the BFKL Green function at small r , resulting in its turn from the nonperturbative rise of the anomalous dimension to unity around the BFKL singularity point. As a result, a large violation of scaling is predicted for the structure function at small x : it grows linearly with Q . This fact will be clearly seen in what follows.

Our second remarks concerns the validity of the expression (12). It has been obtained under the standard assumption that the radius of the strong interaction is much smaller than that of the nucleus. Technically it reduces to the strong inequality

$$\sigma(r)T(b) \ll 1. \quad (23)$$

In fact, if $\sigma(r) \sim r_0^2$, where r_0 is the effective interaction radius, then (23) tells us that $r_0 \ll R_A$. With (19) and (3)-(5) one observes that $\sigma(r)$ can take on large values for light quarks, of the order $1/m_f$, when the standard assumption that the projectile can interact with only one nucleon at a time becomes wrong. However, on physical grounds the expressions (3) and (4) cannot be true for very small values of ϵ_f , which allow for very large values of r . At such distances nonperturbative confinement effects should become notable, which prevent the $q\bar{q}$ pair from having too large dimensions, larger than some maximal possible dimension r_{max} of the order of a typical hadronic size. Then Eq. (23) will always be fulfilled. To simulate the confinement effects we shall substitute the small masses m_f of light quarks by an effective regulator mass $m \sim 1/r_{max}$.

Finally, to simplify the treatment, for $A \gg 1$ and using (23) we can, as usual, transform (12) into an equivalent expression:

$$\sigma_A = 2 \int d^2b \int_0^1 d\alpha \int d^2r \rho(\alpha, r) \{1 - \exp[-(1/2)A\sigma(r)T(b)]\}. \quad (24)$$

3 The nuclear structure function in the limit $x \rightarrow 0$

We begin with the main part of the structure function given by the cross section for the transversal photon. Putting the transversal photon density (4) and the cross section $\sigma(r)$ given by (19) into (24) and changing the variable $r \rightarrow r/\epsilon_f$ we obtain

$$\begin{aligned} \sigma_A^{(T)} &= \frac{2e^2 N_c}{(2\pi)^3} \sum_{f=1}^{N_f} Z_f^2 \int d^2b \int_0^1 d\alpha \int d^2r \\ &\times \left[\frac{m_f^2}{\alpha(1-\alpha)Q^2 + m_f^2} K_0^2(r) + [\alpha^2 + (1-\alpha)^2] K_1^2(r) \right] \left[1 - \exp \left(-\frac{A\mu r R_N T(b)}{2\sqrt{\alpha(1-\alpha)Q^2 + m_f^2}} \right) \right]. \end{aligned} \quad (25)$$

Expression (25) depends on the quark masses m_f . From its form it is evident that the dominant contribution to $\sigma_A^{(T)}$ comes from the region of integration in α where

$$\alpha(1-\alpha)Q^2 < (A\mu R_N/R_A^2)^2 \sim (\nu^\Delta A^{1/3}/R_N)^2. \quad (26)$$

In the asymptotic region $x \rightarrow 0$ and/or $A \gg 1$, to which this and the following sections are devoted, $\nu^\Delta A^{1/3} \gg 1$, so that the right-hand side of (26) is large. Then large values of $\alpha(1-\alpha)Q^2$ will give the dominant contribution, which correspond to small transverse dimensions of the $q\bar{q}$ pair of the order

$$r \sim R_N/(\nu^\Delta A^{1/3}). \quad (27)$$

Evidently the masses m_f do not play any role at such small values of r , so that we can safely put $m_f = 0$ in (25). Then it simplifies to

$$\sigma_A^{(T)} = \frac{2e^2 N_c Z^2}{(2\pi)^3} \int d^2b \int_0^1 d\alpha \int d^2r [\alpha^2 + (1-\alpha)^2] K_1^2(r) \left[1 - \exp\left(-\frac{A\mu r R_N T(b)}{2Q\sqrt{\alpha(1-\alpha)}}\right) \right], \quad (28)$$

where

$$Z^2 = \sum_{f=1}^{N_f} Z_f^2 \quad (29)$$

is the average quark charge squared.

Note that the cross section on the free nucleon follows from (28) in the lowest order in $T(b)$ (and divided by A):

$$\sigma_N^{(T)} = \frac{e^2 N_c Z^2 \mu R_N}{(2\pi)^3 Q} \int_0^1 d\alpha \frac{\alpha^2 + (1-\alpha)^2}{\sqrt{\alpha(1-\alpha)}} \int d^2r r K_1^2(r). \quad (30)$$

Calculating the integrals over α and r ,

$$\sigma_N^{(T)} = \frac{9\pi e^2 N_c Z^2 \mu R_N}{512Q}. \quad (31)$$

It is evident that at high Q the cross section $\sigma_A^{(T)} \simeq A\sigma_N^{(T)}$ so that the EMC effect dies out.

It is instructive to compare the total cross section (28) with separate contributions coming from a given number of interactions n . From (11) we get:

$$\begin{aligned} \sigma_A^{(T,n)} &= -\frac{2e^2 N_c}{(2\pi)^3} C_A^n w_n \sum_{f=1}^{N_f} Z_f^2 \int_0^1 d\alpha \int d^2r \\ &\times \left[\frac{m_f^2}{\alpha(1-\alpha)Q^2 + m_f^2} K_0^2(r) + [\alpha^2 + (1-\alpha)^2] K_1^2(r) \right] \left(-\frac{\mu r R_N}{2\sqrt{\alpha(1-\alpha)Q^2 + m_f^2}} \right)^n. \quad (32) \end{aligned}$$

One observes that all terms except the first one diverge as $m_f \rightarrow 0$. The $n = 1$ term is independent of m_f in this limit and behaves like $1/Q$ (see (31)). Other terms have the order

$$\sigma_A^{(T,2)} \sim Q^{-2} \ln(Q^2/m_f^2), \quad \sigma_A^{(T,n>2)} \sim Q^{-2} m_f^{2-n}. \quad (33)$$

Thus they are all of the same order Q^{-2} with respect to Q and therefore asymptotically smaller than the dominant term with $n = 1$. For the structure function (22) they give contributions essentially independent of Q . In this respect the conclusions in [5] are correct. However comparison to the total cross section (28), which is independent of m_f , demonstrates that the rescattering terms taken separately have little relation to the physical cross section. Evidently all their terms leading in $1/m_f$ cancel in the sum. The final expression (28) does not admit developing in the multiple scattering series.

To simplify the calculation of the cross section (28) we choose a simplified nuclear profile function $T(b)$ corresponding to a finite nucleus with a constant density

$$T(b) = (2/V_A)\sqrt{R_A^2 - b^2}, \quad (34)$$

where $R_A = A^{1/3}R_0$ and V_A is the nuclear volume. Then the integration over b can be done explicitly and we obtain

$$\sigma_A^{(T)} = (2e^2 N_c Z^2 R_A^2 / \pi) J_T, \quad (35)$$

where J_T is given by an integral over α and r :

$$J_T = \int_0^1 d\alpha \int_0^\infty r dr \alpha^2 K_1^2(r) \chi(z). \quad (36)$$

Here

$$\chi(z) = \frac{1}{2} - \frac{1}{z^2} + e^{-z} \left(\frac{1}{z} + \frac{1}{z^2} \right) \quad (37)$$

and

$$z = \frac{3}{4\pi} \frac{A^{1/3} \mu r R_N}{Q R_0^2 \sqrt{\alpha(1-\alpha)}} \equiv z_0 \frac{r}{\sqrt{\alpha(1-\alpha)}}. \quad (38)$$

The cross section for the longitudinal photon can be studied in a similar manner with the colour density given by (3). In the limit $m_f \rightarrow 0$ it is given by a formula analogous to (28):

$$\sigma_A^{(L)} = \frac{8e^2 N_c Z^2}{(2\pi)^3} \int d^2b \int_0^1 d\alpha \int d^2r \alpha(1-\alpha) K_0^2(r) \left[1 - \exp\left(-\frac{A\mu r R_N T(b)}{2Q\sqrt{\alpha(1-\alpha)}}\right) \right], \quad (39)$$

and possesses the same properties and behavior in Q as $\sigma_A^{(T)}$. For a free nucleon the longitudinal cross section turns out to be

$$\sigma_N^{(L)} = \frac{\pi e^2 N_c Z^2 \mu R_N}{256Q}. \quad (40)$$

Finally, with the nuclear profile function chosen according to (34) we obtain

$$\sigma_A^{(L)} = (4e^2 N_c Z^2 R_A^2 / \pi) J_L, \quad (41)$$

where now

$$J_L = \int_0^1 d\alpha \int_0^\infty r dr \alpha(1-\alpha) K_0^2(r) \chi(z), \quad (42)$$

with $\chi(z)$ and z defined by (37) and (38).

According to (35)-(38) and (41),(42) the EMC effect turns out to depend on a single variable z_0 which combines its x -, Q - and A -dependence. Indeed for the ratio $R^{(A)}(x, Q^2)$ of the nuclear structure function per nucleon to the proton one we find

$$R^{(A)}(x, Q^2) \equiv \frac{F_{2A}(x, Q^2)}{A F_{2N}(x, Q^2)} = R(z_0), \quad (43)$$

where, according to (38),

$$z_0 = \frac{3}{4\pi} \frac{A^{1/3} \mu R_N}{QR_0^2} . \quad (44)$$

In principle, z_0 may take on arbitrary values, from very small ones up to very large ones. With the growth of z_0 the effect (i.e., $1 - R^{(A)}$) also grows from zero to unity (Fig. 2). At small z_0 it behaves like $z_0 \ln z_0$ (see Appendix), which corresponds to going down like $\ln Q/Q$ at high Q^2 .

To find physically relevant values of z_0 we note that using (22), (31) and (40) we find the proton structure function:

$$F_{2p}(x, Q^2) = (11/512) N_c Z^2 \mu R_N Q. \quad (45)$$

As mentioned in the Introduction, it exhibits a strong violation of scaling: it rises linearly with Q , which means that the anomalous dimension has risen from its presumably small value up to unity in the asymptotical region. Eq. (45) may be used to express the unknown product μR_N in (44) via $F_{2p}(x, Q^2)$ to relate the parameter z_0 to the observable proton structure function:

$$z_0 = \frac{384}{11\pi} \frac{A^{1/3}}{N_c Z^2 Q^2 R_0^2} F_{2p}(x, Q^2). \quad (46)$$

This allows to calculate the nuclear structure function entirely in terms of the proton one without any unknown parameter,

$$R^{(A)}(x, Q^2) = \frac{2N_c Z^2 R_A^2 Q^2}{\pi^2 A F_{2p}(x, Q^2)} (J_T + 2J_L). \quad (47)$$

Here the integrals $J_{T,L}$ are calculated according to (36) and (42) with z_0 given by (46).

To apply these asymptotic formulas to realistic nuclear structure functions at given x and Q^2 we have first to check that the proton structure function is reasonably well described by the asymptotic expression (45). If we take $\nu \sim 1/x$ in μ (Eq. (21)) then it leads to

$$F_{2p}(x, Q^2) = c \frac{Qx^{-\Delta}}{\sqrt{\ln(1/x)}} , \quad (48)$$

with

$$c = \frac{11\pi}{32} \sqrt{\frac{N_c}{14\zeta(3)}} \frac{N_c^2 - 1}{N_c^2} \alpha_s^{3/2} Z^2 R_N. \quad (49)$$

Comparing (48) with the experimental behaviour of $F_{2p}(x, Q^2)$ one may hopefully determine Δ and c and from (16) and (49) find the parameters α_s and R_N . (Note, however, that the exact scale factor which divides ν in expressions like ν^Δ or $\ln \nu$ cannot be determined in the lowest order BFKL theory. Therefore the linear dependence on Q in (48) may be modified by terms of the order $\alpha_s \ln Q$, which are assumed small in the theory, but are not so small for realistic values of α_s .)

Studying the existing experimental data for $F_{2p}(x, Q^2)$ at low x [14-17], we find that the simple formula (48) describes them quite well for $x < 0.001$ (Fig. 3), with the parameters Δ and c chosen according to

$$\Delta = 0.377, \quad c = 0.0536. \quad (50)$$

They correspond to $\alpha_s = 0.14$ and $R_N = 0.44$ fm. Thus the asymptotic hard pomeron, at least, does not contradict the experimental data for the proton structure function for $x < 0.001$ and leads to physically reasonable values of α_s and R_N . This provides a justification to apply it to the nuclear structure function in the same region.

Taking (48) for F_{2p} and using (46) and (47) with four flavours and $R_0 = 1.35$ fm we have calculated the ratios $R^{(A)}$ for $10^{-6} < x < 10^{-3}$, $Q^2 = 2.5 \div 100$ GeV² and $A = 12 \div 208$. Our results are shown by solid curves in Figs. 4-6, which illustrate the x -, Q - and A -dependence of the EMC effect respectively. The effect rises with $1/x$ due to the rise of F_{2p} , falls with Q as $\ln Q/Q$ and, naturally, rises with A as $A^{1/3}$. Its overall magnitude remains not very large in the whole region explored ($1 - R^{(A)} < 0.5$).

Unfortunately there are no experimental data on the nuclear structure functions at such low x . To be able to compare our results with the existing data, we thus have to move to larger x , where the asymptotic formula (48) does not work.

4 Realistic x and A

In this section we want to consider the region of not so small x and not so large A , where neither the asymptotic form (48) for the proton structure function is valid nor the right-hand side of (26) is large.

The latter condition can easily be taken into account retaining in ϵ_f^2 , Eq. (5), the quark masses squared m_f^2 (with those for the light quarks substituted by the regulator mass squared m^2). Now both terms in ϵ_f (Eq. (5)) become comparable. It means, of course, that now the dominant configurations of the $q\bar{q}$ pair may reach a size of the order $1/m$, i.e., a typically hadronic size.

As to the proton structure function, we have to take into account that its rise with Q becomes considerably slower at not so small x , which implies that the effective anomalous dimension of the pomeron is, in fact, x -dependent and goes down with the growth of x . Of course one may try to study the behaviour of the pomeron at lower energies (higher x) using the BFKL equation with some appropriately chosen boundary conditions (or a driving term). However, since these are poorly known, the resulting predictions are not reliable. Besides, at not too small x subdominant terms in $1/\ln x$ may become essential, which are beyond any control (see however [18], where such terms are introduced from some theoretical considera-

tions). For these reasons, rather than try to determine the subasymptotical behaviour of the pomeron on (poorly known) theoretical grounds, we use a simple extension of the asymptotic formula (48) to finite x which only takes into account a change in the anomalous dimension, to be determined from the comparison to the experimental data. Namely, we assume that the effective anomalous dimension of the pomeron is x dependent and smaller than unity at finite x . Correspondingly we take instead of (19)

$$\sigma(r) = \xi(\nu)(m_N r)^{\beta(\nu)}/m_N^2, \quad (51)$$

where $\beta(\infty) = 1$ and $\beta(\nu) > 1$ at finite ν (perturbatively $\beta \simeq 2$). We have also introduced the nucleon mass m_N in (51) as a natural scale. Evidently as $\nu \rightarrow \infty$ (51) goes into (19) with

$$\xi(\nu) = \mu(\nu)m_N R_N. \quad (52)$$

With the cross section $\sigma(r)$ chosen according to (51) and the quark masses m_f retained, our formulas for the nuclear cross sections (35)-(38), (41) and (42) slightly change because of the flavour dependence. Instead of (35) and (41) we now find

$$\sigma_A^{(T,L)} = (2^n e^2 N_c R_A^2 / \pi) \sum_{f=1}^{N_f} Z_f^2 J_{T,L}^{(f)}, \quad (53)$$

where $n = 1, 2$ for T, L respectively and the integrals $J_{T,L}$, depending on f , are now calculated with

$$z = \frac{\xi(m_N r)^\beta A R_A}{m_N^2 V_A Q^\beta [\alpha(1-\alpha) + m_f^2/Q^2]^{\beta/2}} \equiv z_0 \frac{r^\beta}{[\alpha(1-\alpha) + m_f^2/Q^2]^{\beta/2}} \quad (54)$$

and the factor $\alpha(1-\alpha)$ in (42) substituted as

$$\alpha(1-\alpha) \longrightarrow \frac{[\alpha(1-\alpha)]^2}{\alpha(1-\alpha) + m_f^2/Q^2}. \quad (55)$$

The final EMC ratio $R^{(A)}$ is now calculated according to

$$R^{(A)}(x, Q^2) = \frac{2N_c R_A^2 Q^2}{\pi^2 A F_{2p}(x, Q^2)} \sum_{f=1}^{N_f} Z_f^2 [J_T^{(f)} + 2J_L^{(f)}]. \quad (56)$$

Evidently now it depends on two variables: z_0 defined by (54) and Q^2 .

Calculating the proton structure function with (51) we find instead of (45)

$$F_{2p}(x, Q^2) = (11/512)\lambda N_c \xi(Q/m_N)^{2-\beta}, \quad (57)$$

where λ is a factor resulting from the α and r integrations (and normalized to unity for $\beta = 1$ and $m_f = 0$). To find it one has to calculate the integrals $J_{T,L}$ with the function $\chi(z)$ substituted by its lowest order term $(1/3)z$. If we denote the results $\tilde{J}_{T,L}^{(f)}$, then

$$\lambda = \frac{768}{11\pi^3 z_0} \sum_{f=1}^{N_f} Z_f^2 [\tilde{J}_T^{(f)} + 2\tilde{J}_L^{(f)}]. \quad (58)$$

It is evidently independent of z_0 and can be calculated, say, with $z_0 = 1$.

If we retain the form of $\xi(\nu)$ which follows from (52) then (57) turns into

$$F_{2p}(x, Q^2) = c \frac{Q^{2-\beta(x)} x^{-\Delta}}{\sqrt{\ln(1/x)}} \quad , \quad (59)$$

with c a slowly varying function of $\ln x$, which we take a constant. Choosing at small but finite x the anomalous dimension in the form

$$\gamma(x) = 2 - \beta(x) = 1 + a/\ln x + b/\ln^2 x, \quad (60)$$

we obtain a good agreement with all the experimental data on the proton structure function for $x < 0.05$ [14-17] with the parameters

$$\Delta = 0.237, \quad c = 0.250, \quad a = 3.87, \quad b = 4.62 \quad (61)$$

(see Figs. 7,8). The formulas (59) and (60) then reasonably well extrapolate the asymptotic pomeron to larger values of x , the power $\beta(x)$ taking into account the decrease of the anomalous dimension.

Comparing (54) and (57) we observe that the nuclear structure function can again be written exclusively in terms of the proton one. Indeed the variable z_0 in (54) can be expressed similarly to (46)

$$z_0 = \frac{384}{11\pi\lambda} \frac{A^{1/3}}{N_c Q^2 R_0^2} F_{2p}(x, Q^2), \quad (62)$$

with an extra factor λ in the denominator defined according to (58).

Using (62) and β given by (60) and (61), we have calculated the EMC ratio $R^{(A)}$ for values of $x < 0.05$, $Q^2 > 1 \text{ GeV}^2$ and $A \gg 1$, at which the experimental data are available [19-21]. Four quark flavours have been taken into account (the inclusion of the c quark results important). The value of the internucleon distance has been taken $R_0 = 1.35 \text{ fm}$. The best agreement with the data is achieved for values of the regulator mass m for light quarks of the order of $0.5 \div 1.5 \text{ GeV}$. The results depend very little on m inside this interval: the overall change in $1 - R^{(A)}$ does not exceed 10%. The results for $m = 0.8 \text{ GeV}$ together with the data are presented in the Table. As one observes, a very reasonable agreement is achieved, taking into account that the data, as a rule, are averaged over considerable intervals of x and Q^2 .

At smaller x the behaviour of $R^{(A)}$ with $F_{2p}(x, Q^2)$ given by (59) naturally repeats the one obtained with (48) in the preceding section, except at low Q^2 where the effect of (effective) quark masses is felt. This is illustrated in Figs. 4-6, where the x -, Q - and A -dependence of $R^{(A)}$ calculated with F_{2p} given by (59) is shown by dashed curves, to be compared with the one obtained with (48) (solid curves).

5 Conclusions

As is well known there are serious problems of principle associated with the BFKL hard pomeron, related to the unitarity and the running coupling. In spite of all this, the hard pomeron approach remains the only one, based on first principles, which allows to study low x phenomena, although in a model theory.

As we have found, the hard pomeron, at least, does not contradict the superlow x data for the proton structure function ($x < 0.001$). With some modification the pomeron description can be extended to the region of $x < 0.05$. This gives a motivation to apply it to the nuclear structure function at these x .

With an additional assumption of small interaction between pomerons, which can be justified in the high N_c limit, a closed formula is obtained for the nuclear structure function, expressing it directly in terms of the proton one. For a pure BFKL pomeron and a nucleus of constant density the EMC effect results a function of a single variable z_0 , which combines its x -, Q - and A -dependence. In principle z_0 can take on arbitrary values, so that $R^{(A)}$ can vary from unity to zero. However for realistic x , Q and A the variable z_0 is not so large, so that $R^{(A)}$ remains not very different from unity, except for the lowest x and Q^2 and highest A .

A novel feature of the hard pomeron approach is a changing anomalous dimension. As a result, the behaviour of the EMC effect on Q^2 depends on the value of x . For very small values of x the effect dies out as $\ln Q/Q$. However for larger x the Q -dependence becomes less pronounced until it practically disappears as the anomalous dimension becomes small.

Comparison to the available experimental data for $x < 0.05$ shows a reasonable agreement. The agreement is not ideal, which may be explained partly by the imperfection of the existing data, averaged over considerable intervals of x and Q , partly by the presence of other subasymptotic terms different from the pomeron, which should be notable for not very small x . Evidently more data at lower x are needed to finally conclude about the relevance of the hard pomeron for the EMC effect.

6 Acknowledgements

The authors express their deep gratitude to Prof. Carlos Pajares for his constant interest in the present work and helpful discussions. N.A. and M.A.B. thank the CICYT of Spain and IBERDROLA, respectively, for financial support.

7 Appendix: The asymptotics of the EMC effect at high Q^2

With the quark mass m_f retained and at high Q^2 the EMC ratio $R^{(A)}$ is a function of two small variables, $R^{(A)} = R^{(A)}(z_0, 1/Q^2)$. Since $R^{(A)}(0, 1/Q^2) = 1$ identically, the leading correction term is provided by $R^{(A)}(z_0, 0)$, that is, we can safely put $m_f = 0$ to study it.

The regions of small α and $1 - \alpha$ are responsible for the leading behaviour at $z_0 \rightarrow 0$. Therefore we can limit ourselves with the transversal cross section and consequently with the integral J_T , Eq. (36). Transforming to the integration variable w by

$$\alpha(1 - \alpha) = 1/(w^2 + 4), \quad (63)$$

the dominant contribution will come from large w . Choosing $w_0 \gg 2$, we find that at small z_0

$$J_T \sim 2 \int_0^\infty r dr K_1^2(r) \int_{w_0}^\infty \frac{dw}{w^3} \chi(z), \quad (64)$$

where

$$z = z_0(wr)^\beta, \quad 1 \leq \beta < 2. \quad (65)$$

Passing to the integration over z , we present the right-hand side as

$$J_T \sim (2/\beta) z_0^{2/\beta} \int_0^\infty r^3 dr K_1^2(r) \int_{z_1}^\infty \frac{dz}{z^{1+2/\beta}} \chi(z), \quad (66)$$

with $z_1 = z_0(w_0 r)^\beta$.

The internal integral over z can be transformed into

$$\int_{z_1}^\infty \frac{dz}{z^{1+2/\beta}} \chi(z) = \frac{z_1^{-2/\beta}}{2 + 2/\beta} [\chi(z_1) + (\beta/2) z_1 F(z_1)], \quad (67)$$

where

$$F(z) = \int_1^\infty dx x^{-2/\beta} \exp(-zx) \quad (68)$$

can be expressed via the incomplete gamma function. Evidently the first term in (67) gives a contribution to J_T regular at $z_0 = 0$ and so a correction to $R^{(A)}$ of the order $z_0 \sim 1/Q$. The leading correction comes from the term with $F(z_1)$. Straightforward estimates give that at small z

$$\begin{aligned} F(z) &\sim a + bz^{2/\beta-1}, \quad 1 < \beta < 2; \\ F(z) &\sim a + bz \ln z, \quad \beta = 1. \end{aligned} \quad (69)$$

Putting this into (67) and then into (66) we obtain our final result. At high Q^2

$$\begin{aligned} R^{(A)} &\simeq 1 - c Q^{1-2/\beta}, \quad 1 < \beta < 2; \\ R^{(A)} &\simeq 1 - c \ln Q/Q, \quad \beta = 1. \end{aligned} \quad (70)$$

In particular, with a dimension close to its canonical value $\beta = 2$ the EMC effect results independent of Q .

8 References

1. S.Brodsky, T.E.Close and J.F.Gunion, Phys. Rev. **D6** (1972) 177.
2. S.Brodsky and H.J.Liu, Phys. Rev. Lett. **64** (1990) 1342.
3. N.N.Nikolaev and B.G.Zakharov, Z. Phys. **C49** (1991) 607.
4. V.Barone, M.Genovese, N.N.Nikolaev, E.Predazzi and B.G.Zakharov, Z. Phys. **C58** (1993) 541.
5. B.Z.Kopeliovich and B.Povh, Phys. Lett. **B367** (1996) 329.
6. A.H.Mueller and J.Qiu, Nucl. Phys. **B268** (1986) 427.
7. J.Qiu, Nucl. Phys. **B291** (1987) 746.
8. E.L.Berger and J.Qiu, Phys. Lett. **B206** (1988) 42.
9. V.S.Fadin, E.A.Kuraev and L.N.Lipatov, Phys. Lett. **B60** (1975) 50; I.I.Balitsky and L.N.Lipatov, Sov. J. Nucl. Phys. **15** (1978) 438.
10. G.t'Hooft, Nucl. Phys. **B72** (1974) 461.
11. G.Veneziano, Phys. Lett. **B52** (1974) 220; Nucl. Phys. **B117** (1976) 519.
12. M.A.Braun, Univ. of St. Petersburg preprint SPbU-IP-1995/3 (hep-ph/9502403) (to be published in Z. Phys. **C**).
13. L.N.Lipatov, in *Perturbative Quantum Chromodynamics*, Ed. A.H.Mueller, Advanced Series on Directions in High Energy Physics, World Scientific, Singapore 1989.
14. NM Collab., P.Amaudruz et al., Phys. Lett. **B295** (1992) 159.
15. ZEUS Collab., M.Derrick et al., Z. Phys. **C69** (1996) 607.
16. ZEUS Collab., M.Derrick et al., Z. Phys. **C65** (1995) 379.
17. H1 Collab., T.Ahmed et al., Nucl. Phys. **B439** (1995) 471.
18. J.Kwieciński, A.D.Martin and P.J.Sutton, Univ. of Durham preprint DTP/96/02 (hep-ph/9602320).
19. E665 Collab., M.R.Adams et al., Phys. Rev. Lett. **22** (1992) 3266.
20. EM Collab., J.Ashman et al., Z. Phys. **C57** (1993) 211.
21. NM Collab. M.Arneodo et al., Nucl. Phys. **B441** (1995) 5; 12.

Table

EMC ratios at experimentally known points.

A	x	Q^2 GeV ²	R	R_{exp}	Ref
131	0.0065	1.34	0.780	0.840 ± 0.107	[19]
131	0.0095	1.91	0.825	0.800 ± 0.108	[19]
131	0.0210	3.58	0.889	0.900 ± 0.110	[19]
64	0.0310	4.50	0.925	0.930 ± 0.033	[20]
64	0.0500	8.50	0.955	0.955 ± 0.028	[20]
64	0.0150	4.50	0.923	0.857 ± 0.032	[20]
64	0.0310	3.30	0.904	0.963 ± 0.022	[20]
64	0.0500	6.40	0.944	1.005 ± 0.018	[20]
12	0.0055	1.10	0.861	0.904 ± 0.013	[21]
12	0.0085	1.60	0.894	0.939 ± 0.012	[21]
12	0.0125	2.20	0.917	0.939 ± 0.009	[21]
12	0.0175	2.90	0.934	0.957 ± 0.010	[21]
12	0.0250	3.60	0.945	0.963 ± 0.009	[21]
12	0.0350	4.50	0.954	0.990 ± 0.009	[21]
12	0.0450	5.50	0.962	0.983 ± 0.010	[21]
40	0.0085	1.40	0.840	0.846 ± 0.014	[21]
40	0.0125	1.90	0.871	0.870 ± 0.011	[21]
40	0.0175	2.50	0.895	0.908 ± 0.011	[21]
40	0.0250	3.40	0.917	0.946 ± 0.009	[21]
40	0.0350	4.70	0.937	0.956 ± 0.009	[21]
40	0.0450	5.70	0.946	0.986 ± 0.011	[21]

Figure captions

Fig. 1. Pomeron diagrams for the EMC effect in the leading approximation in $1/N_c$. With a small coupling constant the diagram (a) dominates at large energies.

Fig. 2. EMC effect as a function of the parameter z_0 (Eq. (44)).

Fig. 3. The pomeron fit (48),(50) to the proton structure function for $x < 0.001$ compared to the experimental data [14-17] at $Q^2 = 3, 12$ and 35 GeV^2 .

Fig. 4. The x -dependence of the EMC effect calculated with the proton structure function described by the pure pomeron (Eq. (48), solid curves) and the subasymptotic pomeron (Eq. (59), dashed curves) for $x < 0.001$, $A = 64$ and $Q^2 = 3$ and 50 GeV^2 .

Fig. 5. The Q^2 -dependence of the EMC effect calculated with the proton structure function described by the pure pomeron (Eq. (48), solid curves) and the subasymptotic pomeron (Eq. (59), dashed curves) for $A = 64$ and $x = 10^{-3}$ and 10^{-6} .

Fig. 6. The A -dependence of the EMC effect calculated with the proton structure function described by the pure pomeron (Eq. (48), solid curves) and the subasymptotic pomeron (Eq. (59), dashed curves) for $x = 10^{-3}$ and 10^{-6} and $Q^2 = 10 \text{ GeV}^2$.

Fig. 7. The subasymptotic pomeron fit (59)-(61) to the proton structure function for $x < 0.05$ compared to the experimental data [14-17] at $Q^2 = 3, 12$ and 35 GeV^2 .

Fig. 8. The effective anomalous dimension $\gamma = 2 - \beta$ as a function of x (Eqs. (60),(61)).

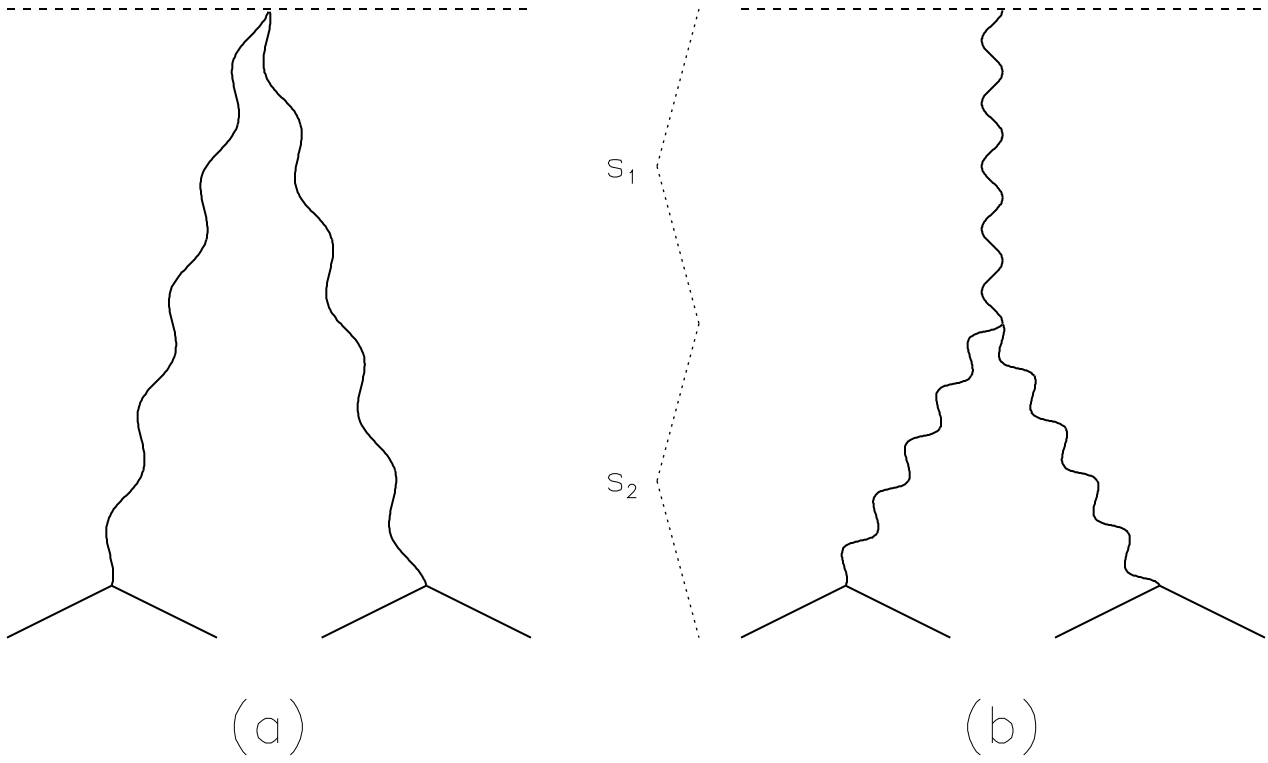


Fig. 1

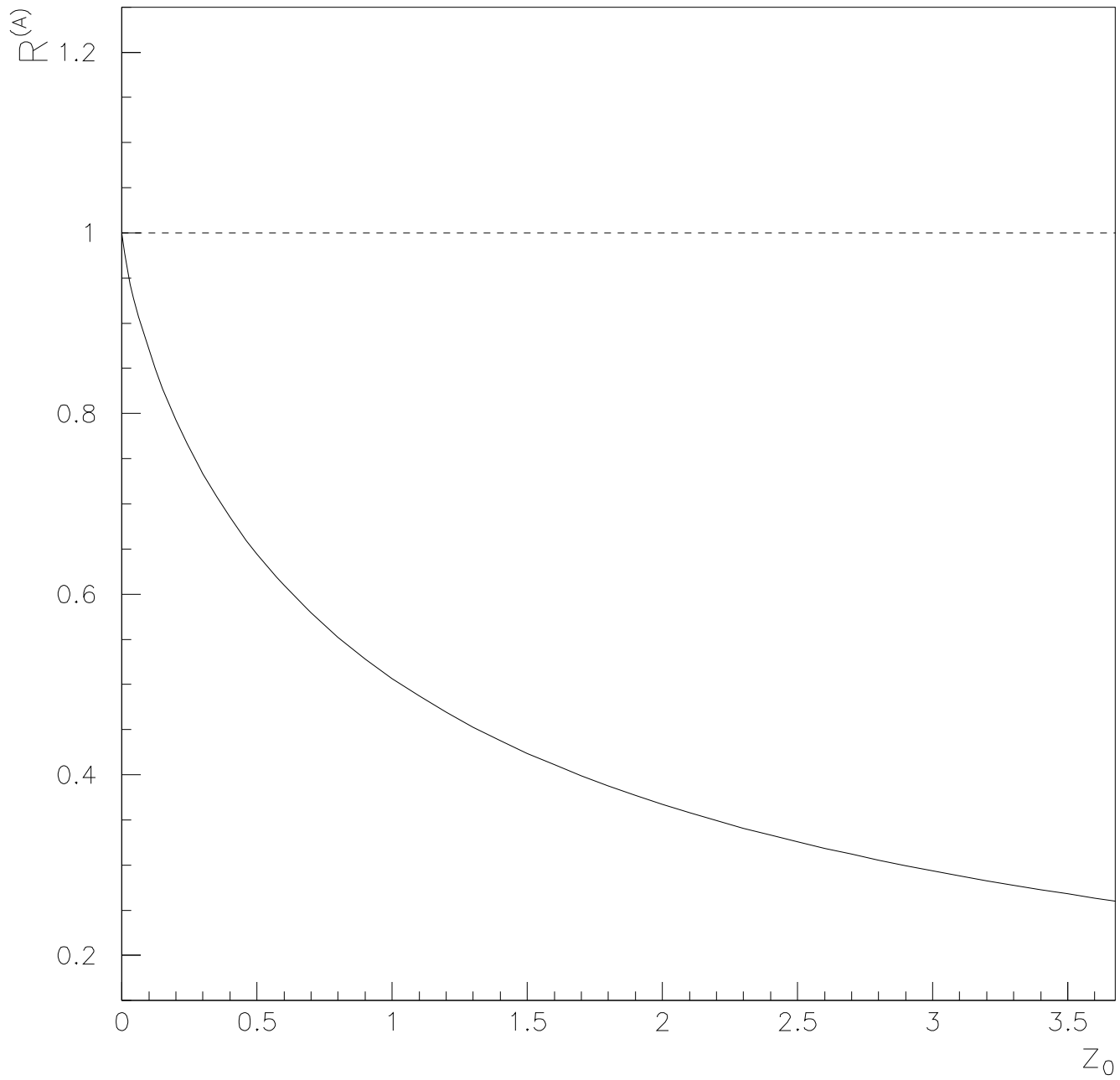


Fig. 2

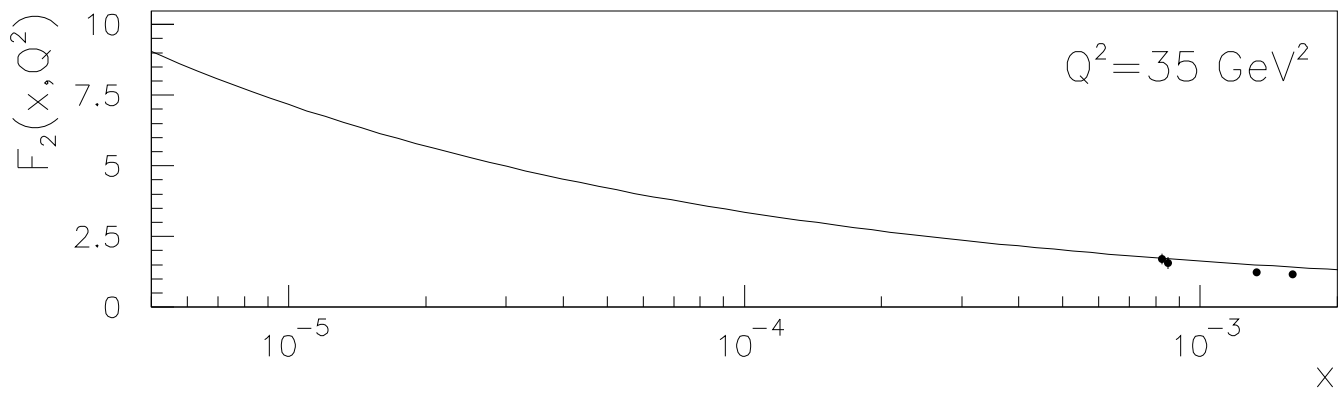
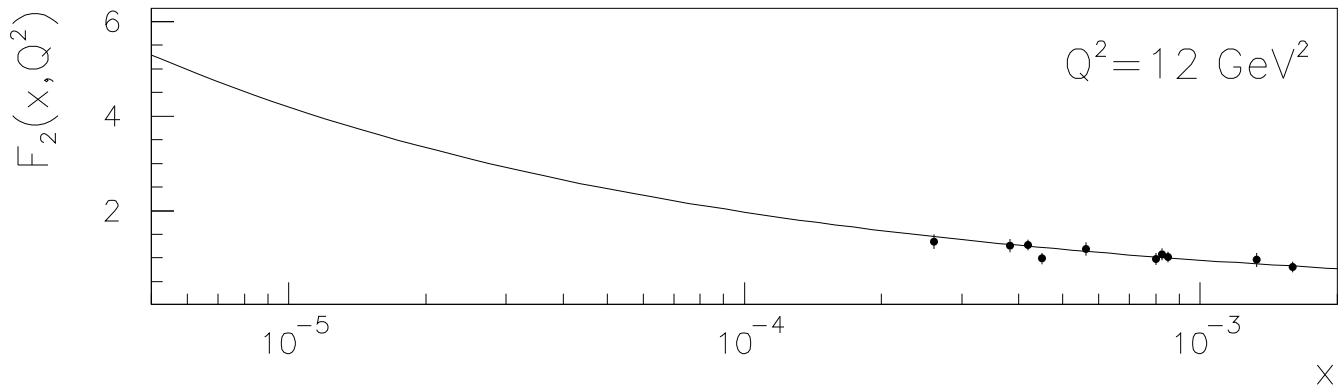
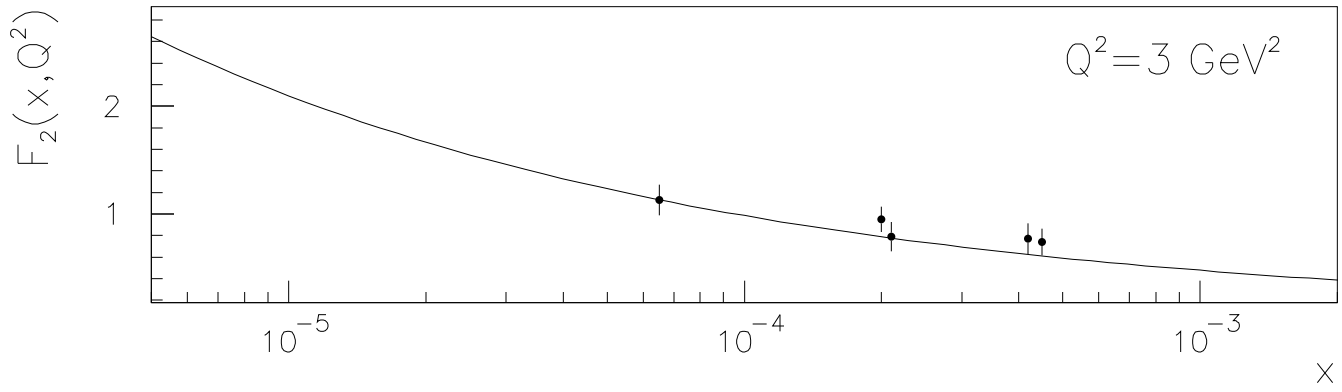


Fig. 3

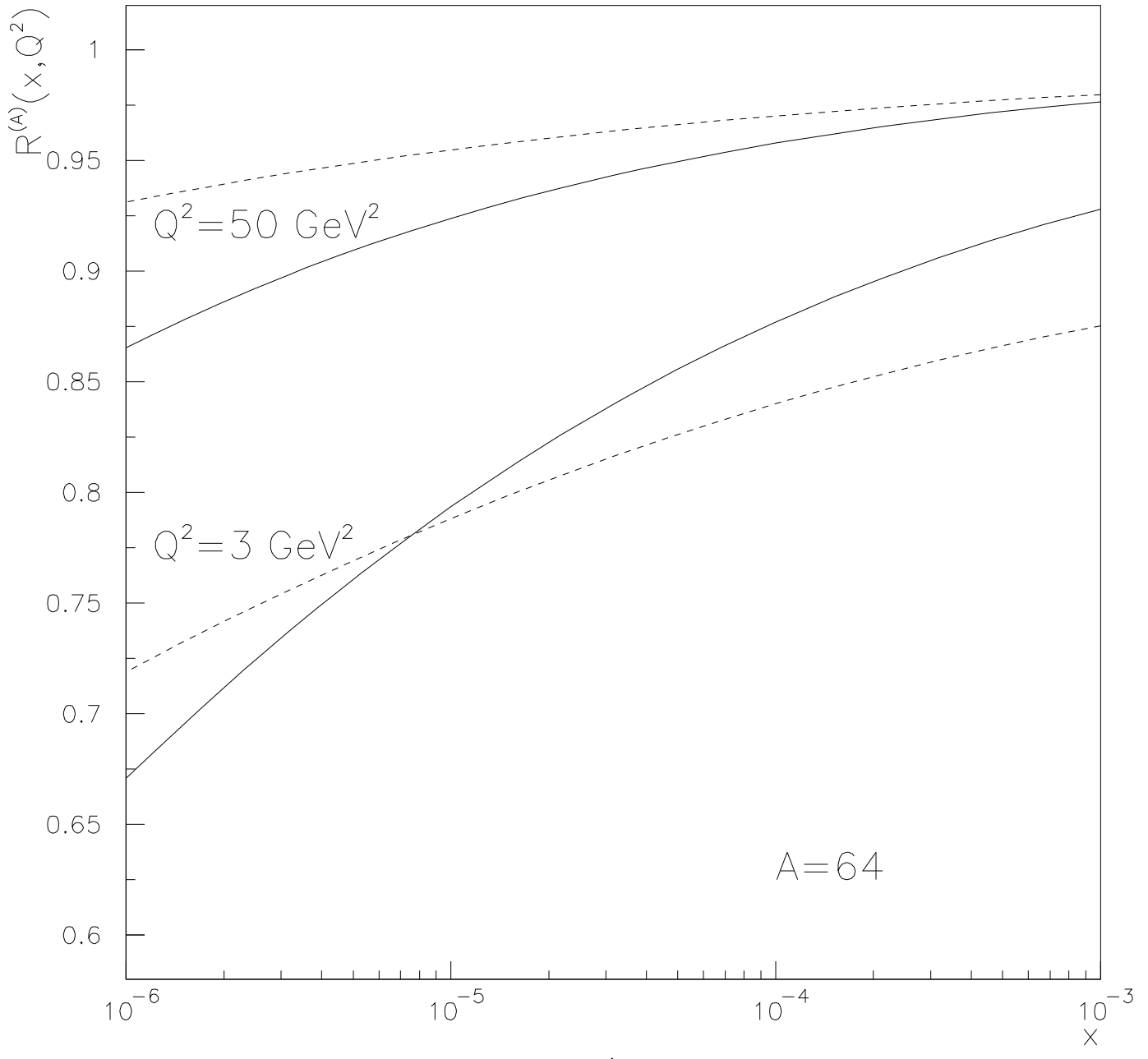


Fig. 4

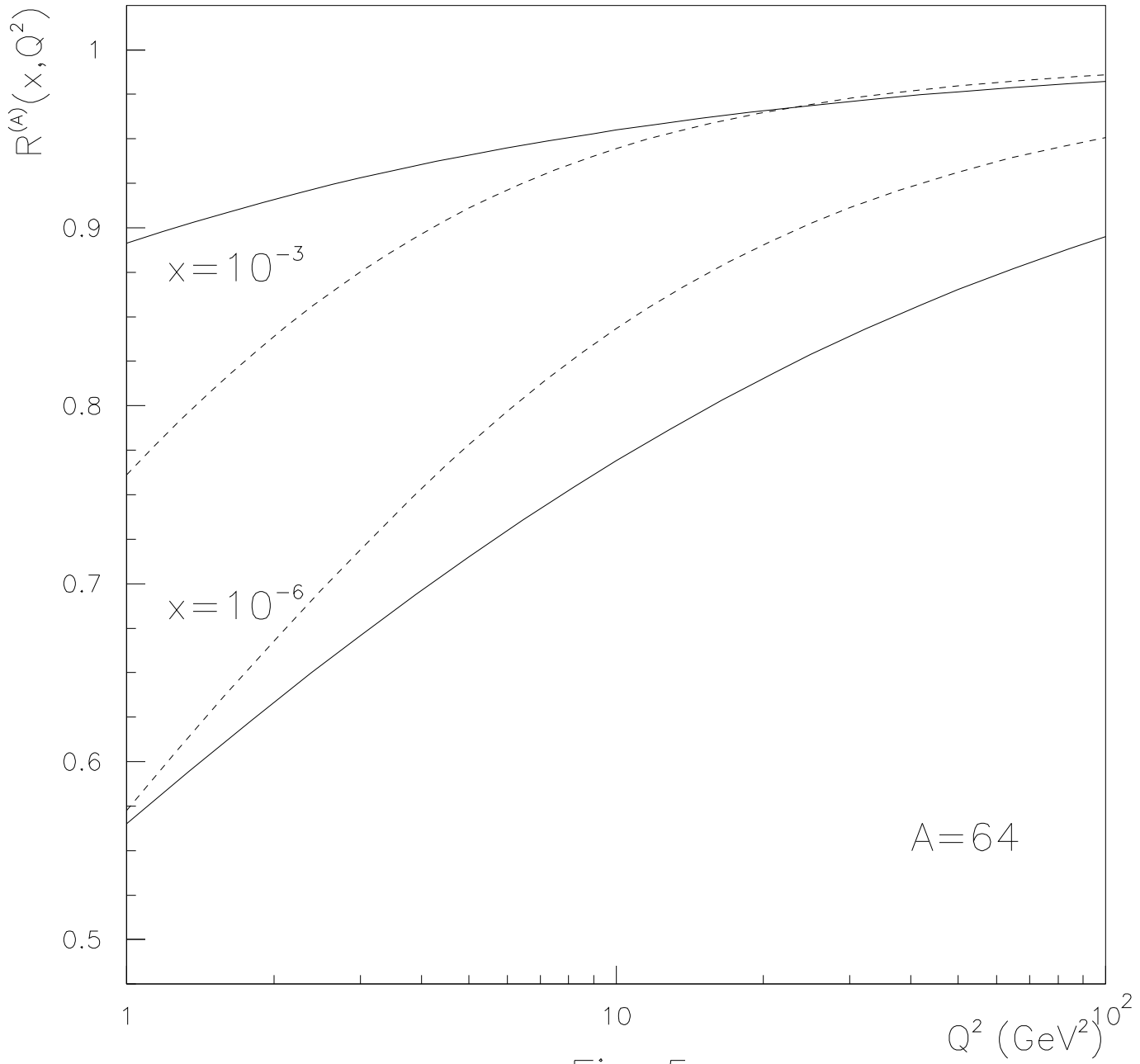


Fig. 5

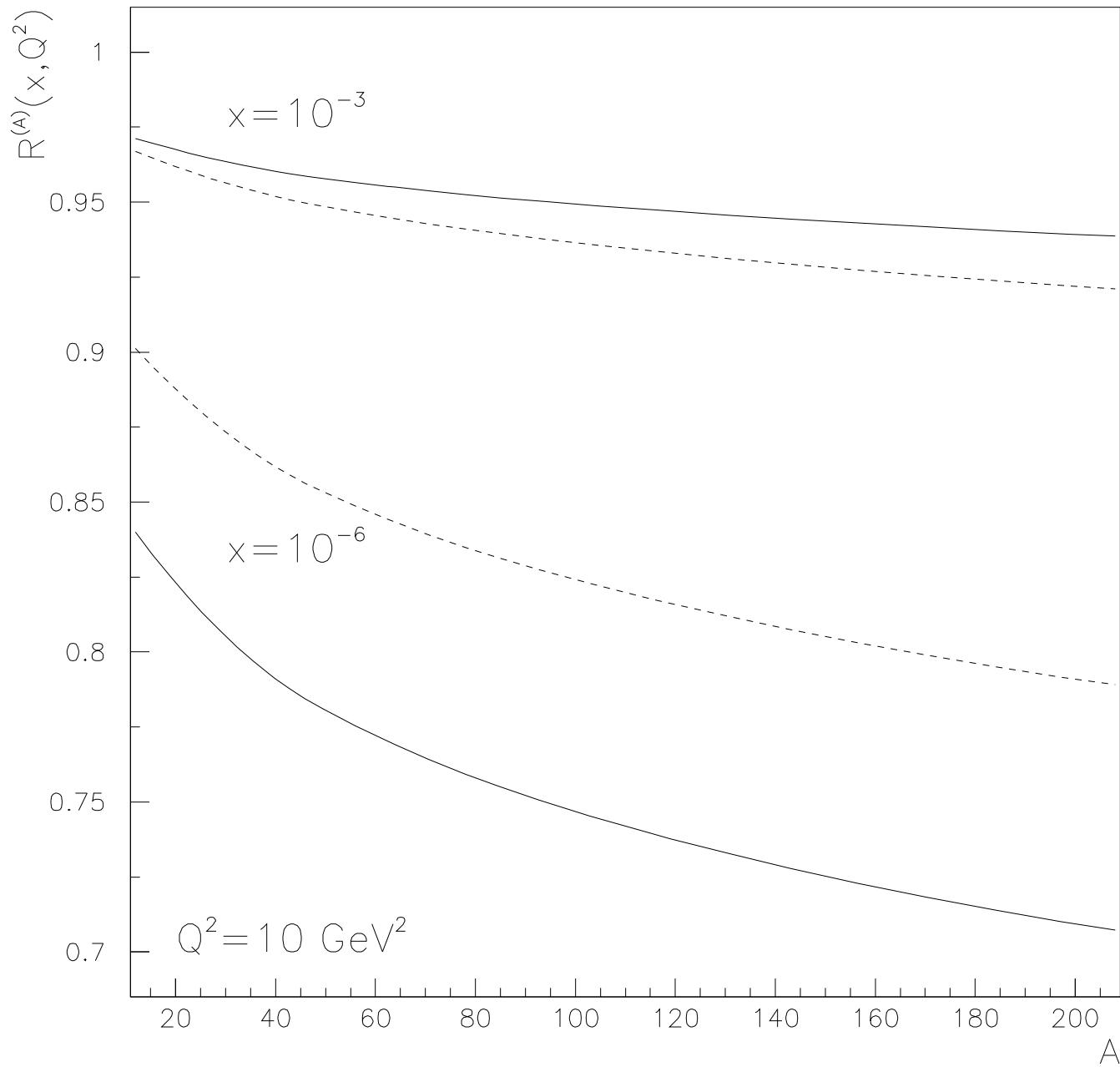


Fig. 6

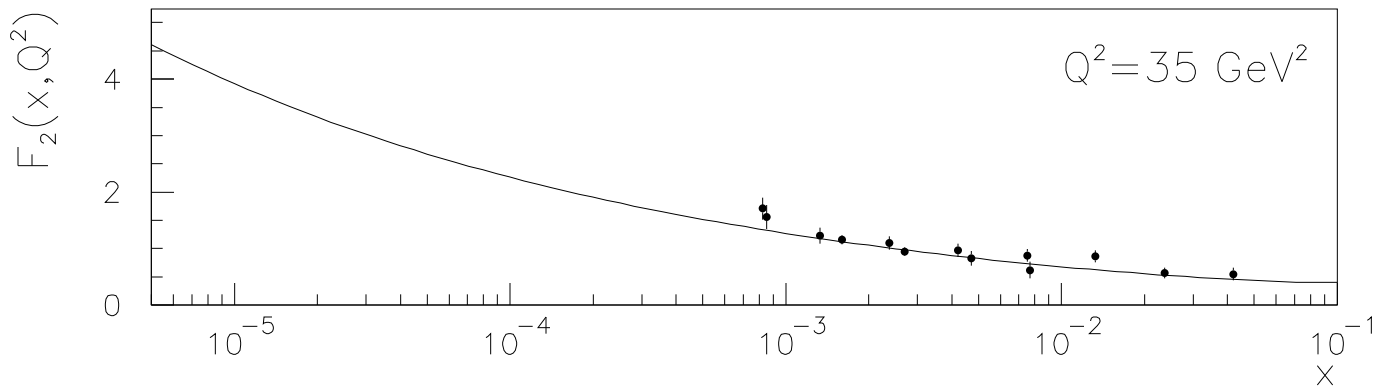
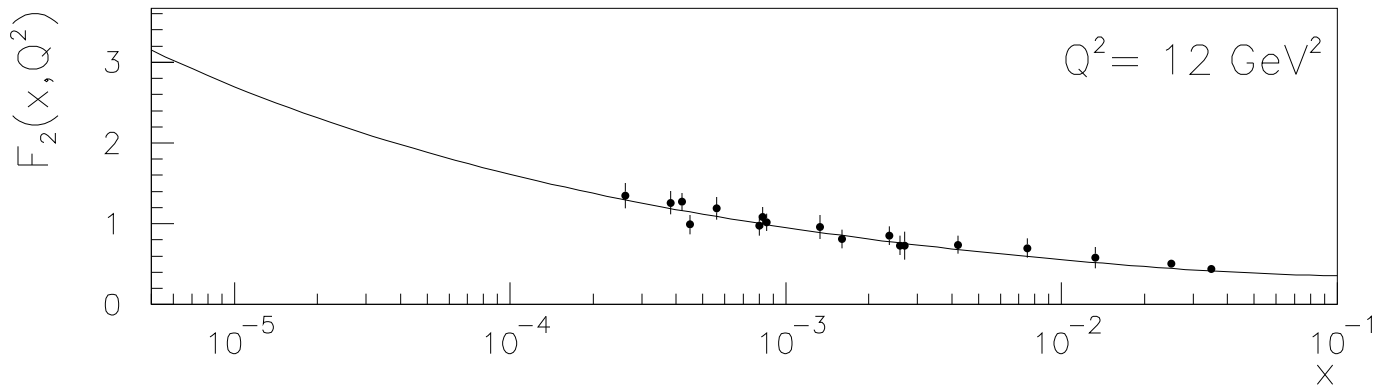
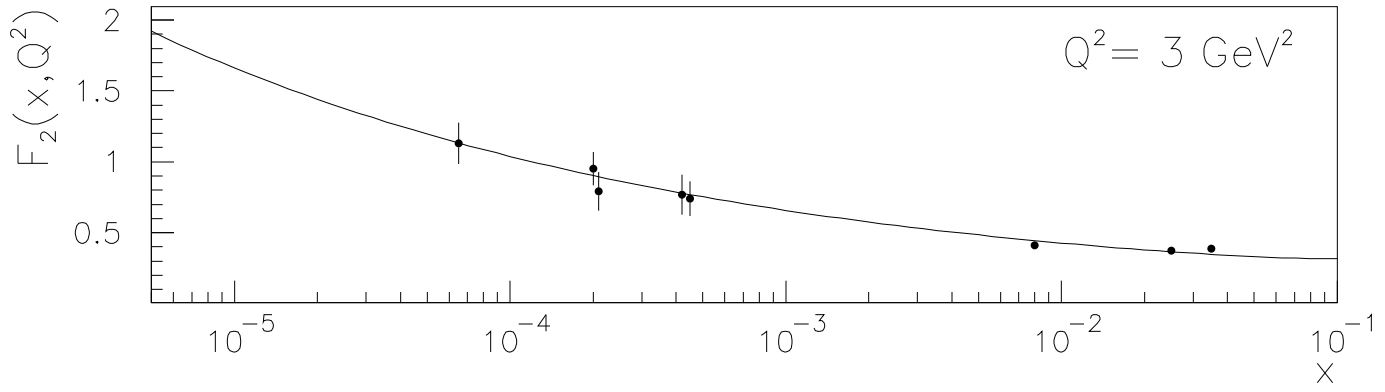


Fig. 7

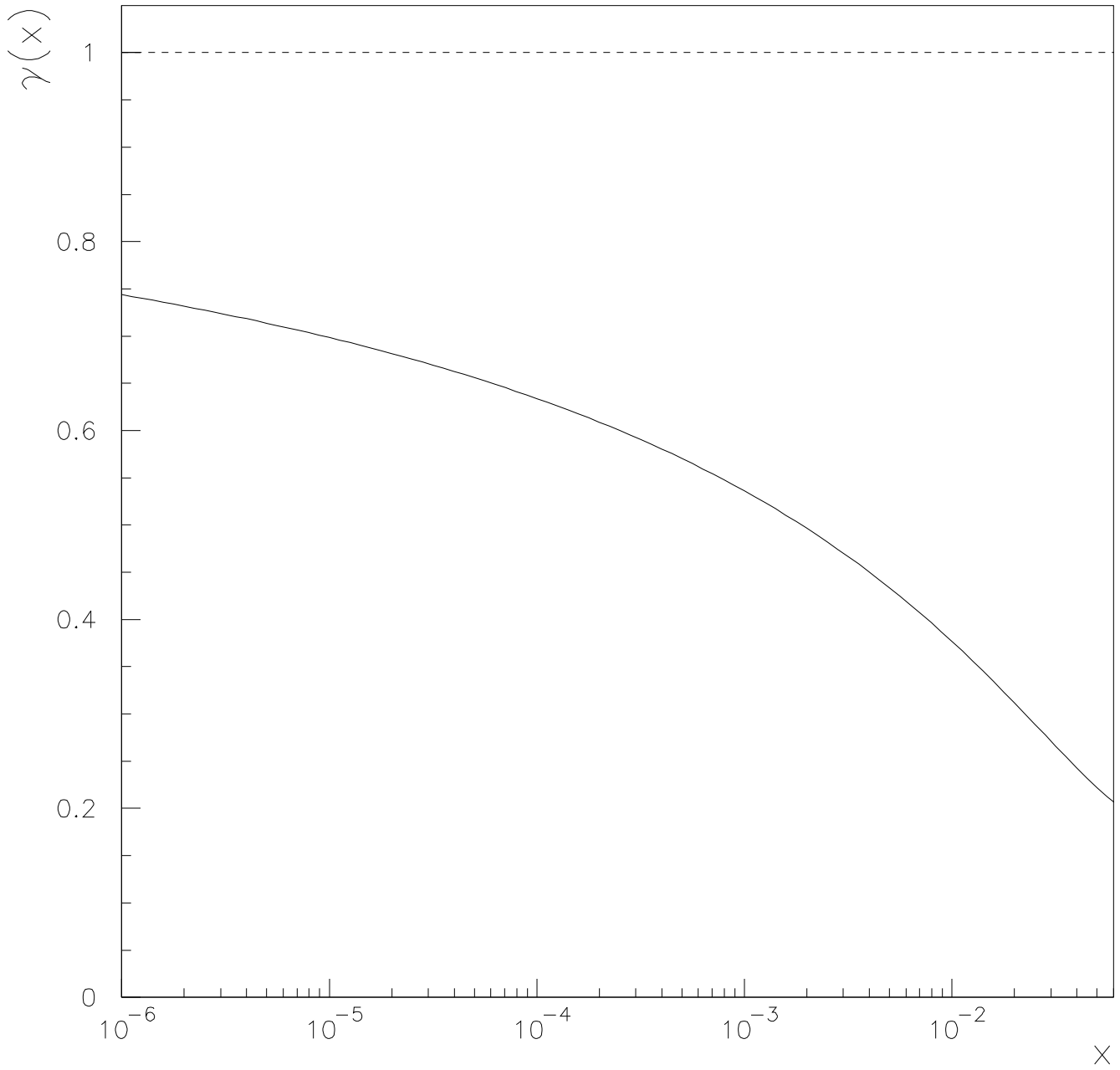


Fig. 8